Error Control Coding in Low-Power Wireless Sensor Networks: When Is ECC Energy-Efficient?

Article *in* EURASIP Journal on Wireless Communications and Networking · December 2006

DOI: 10.1155/WCN/2006/74812 · Source: DBLP

3 authors:

Sheryl L Howard
Northern Arizona University
16 PUBLICATIONS **450** CITATIONS
SEE PROFILE

Christian Schlegel
Dalhousie University
299 PUBLICATIONS **4,582** CITATIONS
SEE PROFILE

K. Iniewski
CMOS Emerging Technologies Research
220 PUBLICATIONS **2,220** CITATIONS
SEE PROFILE

Hindawi Publishing Corporation
EURASIP Journal on Wireless Communications and Networking
Volume 2006, Article ID 74812, Pages 1–14
DOI 10.1155/WCN/2006/74812

Error Control Coding in Low-Power Wireless Sensor Networks: When Is ECC Energy-Efficient?

Sheryl L. Howard, Christian Schlegel, and Kris Iniewski

Department of Electrical & Computer Engineering, University of Alberta, Edmonton, AB, Canada T6G 2V4

Received 31 October 2005; Revised 10 March 2006; Accepted 21 March 2006

This paper examines error control coding (ECC) use in wireless sensor networks (WSNs) to determine the energy efficiency of specific ECC implementations in WSNs. ECC provides coding gain, resulting in transmitter energy savings, at the cost of added decoder power consumption. This paper derives an expression for the critical distance d_{CR}, the distance at which the decoder's energy consumption per bit equals the transmit energy savings per bit due to coding gain, compared to an uncoded system. Results for several decoder implementations, both analog and digital, are presented for d_{CR} in different environments over a wide frequency range. In free space, d_{CR} is very large at lower frequencies, suitable only for widely spaced outdoor sensors. In crowded environments and office buildings, d_{CR} drops significantly, to 3 m or greater at 10 GHz. Interference is not considered; it would lower d_{CR}. Analog decoders are shown to be the most energy-efficient decoders in this study.

1. INTRODUCTION

Wireless sensor networks are currently being considered for many communications applications, including industrial, security surveillance, medical, environment and weather monitoring, among others. Due to limited embedded battery lifetime at each sensor node, minimizing power consumption in the sensors and processors is crucial to successful and reliable network operation. Power and energy efficiency is of paramount interest, and the optimal WSN design should consume the minimum amount of power needed to provide reliable communication. New approaches in transmitter and system design have been proposed to lower the required power in the sensor network [1–14].

Error control coding (ECC) is a classic approach used to increase link reliability and lower the required transmitted power. However, lowered power at the transmitter comes at the cost of extra power consumption due to the decoder at the receiver. Stronger codes provide better performance with lower power requirements, but have more complex decoders with higher power consumption than simpler error control codes. If the extra power consumption at the decoder outweighs the transmitted power savings due to using ECC, then ECC would not be energy-efficient compared with an uncoded system.

Previous research using ECC in wireless sensor networks focused primarily on longtime industry-standard codes such as Reed-Solomon and convolutional codes. A hybrid scheme choosing the most energy-efficient combination of ECC and ARQ is considered in [15], using checksums, CRCs, Reed-Solomon and convolutional codes. A predictive error-correction algorithm is presented in [16] which uses data correlation, but is not an error control code, as there is no encoding. Power-aware, system-level techniques including modulation and MAC protocals, as well as differing rate and constraint length convolutional coding, are considered in [17] to reduce system energy consumption in wireless microsensor networks. Depending on the required bit error rate (BER), a higher rate convolutional code, or no coding at all, could be the most energy-efficient approach.

This paper examines several different decoder implementations for a range of ECC types, including block codes, convolutional codes, and iteratively decoded codes such as turbo codes [18] and low-density parity-check codes (LDPCs) [19]. Both digital and analog implementations are considered. Analog implementations seem a natural choice for low-power applications due to their minimal power consumption with subthreshold operation.

Decoder power consumption is compared to coding gain and energy savings at the transmitter for each decoder implementation to determine at what distance use of that decoder becomes energy-efficient. Different environments and a range of frequencies are considered. Our initial work in

[20, 21] is extended to a more realistic power consumption model, and transmitter efficiency is considered as well. Equations for the critical distance d_{CR}, where energy expenditure per data bit is equivalent for the coded and uncoded system, are developed and presented for both high and low throughput channels. At distances greater than d_{CR}, use of the coded system results in net energy savings for a WSN.

Section 2 of this paper presents a framework for the factors that affect the minimum transmitter power, and a path loss model. Basic types of ECC are presented in Section 3. Section 4 explores the energy savings from ECC in terms of coding gain, presents models for the power consumption of a decoder at high and low throughput, and develops equations for the total energy savings, combining transmit energy savings with decoder energy cost, and for the critical distance d_{CR}. The critical distances for actual decoder implementations are found in Section 5 for several different environments and frequencies. Conclusions based on these results are presented in Section 6.

2. TRANSMITTED POWER AND PATH LOSS

2.1. Minimum transmitted power

Minimizing transmitted RF power is the key to energy-efficient wireless sensor networks [1–3]. To shed more light on RF transmission power, let us consider that the receiver has a required minimum signal-to-noise power S/N, below which it cannot operate reliably. Often, this requirement is expressed in terms of minimum E_b/N_0, where E_b is the required minimum energy per bit at the receiver, and N_0 is the noise power spectral density. The S/N can be found as [22]

$$\frac{S}{N} = \frac{RE_b}{N_0 B} = \eta \frac{E_b}{N_0}, \tag{1}$$

where R is the information rate or throughput in bps, B is the signal bandwidth, and η, the ratio of the information rate to the bandwidth, is known as the spectral efficiency.

The signal noise N may be expressed as proportional to thermal noise and the signal bandwidth B, as [23]

$$N = mkTB, \tag{2}$$

where m is a noise proportionality constant, k is the Boltzmann constant, and T is the absolute temperature in K. The receiver noise figure RNF in dB is incorporated into the proportionality constant m such that $m \geq 1$ and $m = 10^{\mathrm{RNF}/10}$. An ideal receiver with RNF = 0 dB results in $m = 1$.

Finally, the received signal power $S_{RX} = S$ at a distance d from the transmitting source can be expressed in free space using the Friis transmission formula [24], assuming an omnidirectional antenna and no interference or obstacles,

$$S_{RX} = \left(\frac{1}{4\pi d^2}\right)\frac{\lambda^2}{4\pi} P_{TX}, \tag{3}$$

where λ is the transmitted wavelength corresponding to the transmitting frequency f with $\lambda = c/f$, and P_{TX} is the transmitted power.

Equations (1), (2), and (3) may be combined to express the minimum transmitted power P_{TX} required to achieve S/N at a receiver a distance d away, in free space, without interference, as

$$P_{TX} = \frac{S}{N} N \left(\frac{4\pi d}{\lambda}\right)^2,$$
$$P_{TX} = \eta \frac{E_b}{N_0} mkTB \left(\frac{4\pi d}{\lambda}\right)^2. \tag{4}$$

Note that in (4) the minimum transmitted power is proportional to distance squared, d^2, between transmitter and receiver, and inversely proportional to λ^2, which means the power is proportional to frequency f. Operation at higher frequencies requires higher transmit power.

Section 2.2 considers the effect of transmitting in an environment which is not free space. Many transmission environments include significant obstacles, and interference, and have reduced line-of-sight (LOS) components. Signal path loss or attenuation in these environments can be significantly greater than that in free space. We will not consider external sources of interference in these environments; only structural interference by obstacles such as walls, doors, furniture, and carpeted wall dividers is considered.

2.2. Path loss modeling

The Friis transmission formula is rewritten below in a different form, as (7) is a well-known formula for RF transmission in a free space in a far-field region [24]. Since wireless sensors are likely to be deployed in a number of different, physically constrained environments, it is worthwhile exploring its limitations. The space surrounding a radiating antenna is typically subdivided into three different regions [24]:

(i) reactive near field,
(ii) radiating near field (Fresnel region),
(iii) far field (Fraunhofer region).

As the Friis formula applies to the far-field region, it is important to establish a minimum distance d_{ff} where the far field begins, and beyond which (3) and (7) are valid. The physical definition of the far-field is the region where the field of the antenna is essentially independent of the distance from the antenna. If the antenna has a maximum dimension D, the far-field region is commonly recognized to exist if the sensor separation d is larger than [24]

$$d > d_{ff} = \frac{2D^2}{\lambda}. \tag{5}$$

While sensor nodes can use different kinds of antennas depending on cost, application, and frequency of operation, a first-order estimate of the antenna size D can be assumed as λ/L, where L is an integer whose value is dependent on antenna design. The above assumption expresses a common

relationship between antenna size and the corresponding radiating wavelength λ. Substituting $D = \lambda/L$ into (5), the distance limitation can be expressed as

$$d > d_{\text{ff}} = \frac{2}{L^2}\lambda. \tag{6}$$

Typical frequencies used in RF transmission vary from as low as 400 MHz (Medical Implant Communications Service—MICS) to 10 GHz (highest band of ultra-wideband technology) with many services offered around 2.4 GHz (Bluetooth, Wireless LAN—802.11, some cellular phones). The corresponding wavelengths change from 75 cm (at 400 MHz) down to 33 mm (at 10 GHz). As a result, the limitations imposed by (6) seem not too restrictive, as even at the lowest frequencies, with largest wavelength, d_{ff} will be below 1 m.

Even if one does not assume proportionality between the antenna size D and wavelength λ, it would be straightforward to calculate the minimum distance d_{ff} directly from (5). For practical reasons due to size limitation, the antenna should not be much larger than the sensor node hardware itself, which in turn should not be larger than a few cubic centimeters. As a result, D should not be larger than 10 cm, resulting in d_{ff} of a fraction of a meter at most.

In further deliberations, we will assume that the distance between sensors is at least 1 meter, which places both corresponding antennas between the receiver and transmitter in the far-field region. The results of Section 5.1 regarding the distance at which ECC becomes energy-efficient for various decoder implementations will justify this assumption.

Equation (3) can be written as

$$\text{PL}(d) = \frac{S_{\text{RX}}(d)}{P_{\text{TX}}} = \left(\frac{4\pi d}{\lambda}\right)^2, \tag{7}$$

where PL is a path loss, which is the loss in signal power at a distance d due to attenuation of the field strength. In a log scale, (7) becomes [25]

$$\text{PL}(d) = \text{PL}(d_0) + 10n\log_{10}\left(\frac{d}{d_0}\right), \tag{8}$$

where $n = 2$. Later this equation is generalized to include other values of n, which better fit the measured attenuation of environments which are more cluttered or confined than the free space assumption:

(i) n = mean path loss exponent ($n = 2$ for free space),
(ii) d_0 = reference distance = 1 m,
(iii) d = transmitter-receiver separation (m) and the reference path loss at d_0 is given by

$$\text{PL}(d_0) = 20\log_{10}\left(\frac{4\pi d_0}{\lambda}\right), \tag{9}$$

(iv) λ = the wavelength of the corresponding carrier frequency f.

The second, more important, limitation of the Friis transmission formula results from the free space propagation assumption. In reality for practically deployed wireless sensor networks, it is unlikely that this assumption will remain valid. Small antennas causing Fresnel zone losses, multiple objects blocking line of sight, or walls and ceilings in indoor environments will all cause deviations from the simple prediction of (7).

Various models have been developed over the years to improve the accuracy of (7) under different conditions [26–29]. Recently a path loss model based on the geometrical properties of a room was presented in [30]. The authors derived equations for the upper and lower bounds of the mean received power (MRP) of a transmission in the room, for random transmitter and receiver locations. Although mathematically complex, these equations fail to reproduce the experimental data of [30]. In fact, the simple equation (7) seems to provide better accuracy. However, the problem with (7) is that it does not take into account losses caused by transmission through walls, reflections from ceilings and Fresnel zone blockage effects. In order to account for some of these effects, one model [31] proposes to apply an additional correction factor in the form of a linear (on a log scale) attenuation factor, in addition to the value predicted by (7). The additional attenuation factor ranges from 0.3 to 0.6 dB/m depending on selected frequency.

To retain generality but keep the path loss equation simple, we will follow many others [25, 26, 32, 33], in assuming the form of (8) with n being an empirically fitted parameter depending on the environment. For free space conditions, $n = 2$ as stated by the Friis transmission formula (7). In real deployment conditions, attenuation loss with distance d will increase more than the squared response implied by (7). To accommodate a wide variety of conditions, the path loss exponent in (3) can be changed from $n = 2$ up to $n = 4$, with $n = 3$ being a typical value when walls and floors are being considered.

Under special conditions, the coefficient n might lie outside the 2–4 range; for example, for short distance line-of-sight paths, the path loss exponent can be below $n = 2$ [26]. This is especially true in hallways, as they provide a waveguiding effect. In other conditions, $n > 4$ has been suggested if multiple reflections from various objects are considered. In the following section, we will assume the validity of (8) with a value of n in the range from $n = 2$ to $n = 4$, with $n = 3$ being representative of most typical indoor environments and outdoor urban/suburban foliated areas [34]. Dense outdoor urban environments can have $n \geq 4$ [35].

3. ERROR CONTROL CODING

Error control coding (ECC) introduces redundancy into an information sequence $\mathbf{u}$ of length k by the addition of extra parity bits, based on various combinations of bits of $\mathbf{u}$, to form a codeword $\mathbf{x}$ of length $n_C > k$. The redundancy provided by these extra $n_C - k$ parity bits allows the decoder to possibly decode noisy received bits of $\mathbf{x}$ correctly which, if uncoded, would be demodulated incorrectly. This ability to correct errors in the received sequence means that use of ECC over a noisy channel can provide better bit error rate (BER) performance for the same signal-to-noise ratio (SNR) compared to an uncoded system, or can provide the same BER at

a lower SNR than uncoded. This difference in required SNR to achieve a certain BER for a particular code and decoding algorithm compared to uncoded is known as the *coding gain* for that code and decoding algorithm.

Typically there is a tradeoff between coding gain and decoder complexity. Very long codes provide higher gain but require larger decoders with high power consumption, and similarly for more complex decoding algorithms.

Several different types of ECC exist, but we may loosely categorize them into two divisions: (1) block codes, which are of a fixed length n_C, with $n_C - k$ parity bits, and are decoded one block or codeword at a time; (2) convolutional codes, which, for a rate k/n_C code, input k bits and output n_C bits at each time interval, but are decoded in a continuous stream of length $L \gg n_C$. Block codes include repetition codes, Hamming codes [36], Reed-Solomon codes [37], and BCH codes [38, 39]. The terminology (n_C, k) or $(n_C, k, d_{\min})$ indicates a code of length n_C with information sequence of length k, and minimum distance (the minimum number of different bits between any of the codewords) $d_{\min}$. Short block codes like Hamming codes can be decoded by syndrome decoding or maximum likelihood (ML) decoding by either decoding to the nearest codeword or decoding on a trellis with the Viterbi algorithm [40] or maximum a posteriori (MAP) decoding with the BCJR algorithm [41]. Algebraic codes such as Reed-Solomon and BCH codes are decoded with a complex polynomial solver to determine the error locations. Convolutional codes are decoded on a trellis using either Viterbi decoding, MAP decoding, or sequential decoding.

Another categorization is based on the decoding algorithms: (1) noniterative decoding algorithms, such as syndrome decoding for block codes or maximum likelihood (ML) nearest-codeword decoding for short block codes, algebraic decoding for Reed-Solomon and BCH codes, and Viterbi decoding or sequential decoding for convolutional codes; (2) iterative decoding algorithms, such as turbo decoding with component MAP decoders for each component code, and the sum-product algorithm (SPA) [42] or its lower complexity approximation, min-sum decoding [43, 44], for low-density parity-check codes (LDPCs).

The noniterative decoding category may be further divided into hard- and soft-decision decoders; hard-decision decoders output a final decision on the most likely codeword, while soft-decision decoders provide soft information in the form of probabilities or log-likelihood ratios (LLRs) on the individual codeword bits. Viterbi decoding can be either hard-decision or soft-decision, with a 2 dB gain in performance for soft-decision decoding. Category (2) are all soft-decision algorithms by nature, as iterative decoding requires soft information as a priori input for each iteration. Iterative decoding algorithms provide significant coding gain, at the cost of greater decoding complexity and power consumption.

Figure 1 shows BER performance versus SNR for several types of error-correcting codes, compared to uncoded BPSK (binary phase-shift keying) modulation. Transmission is over an additive white Gaussian noise (AWGN) channel, with variance $N_0/2$ and zero mean, using BPSK modulation

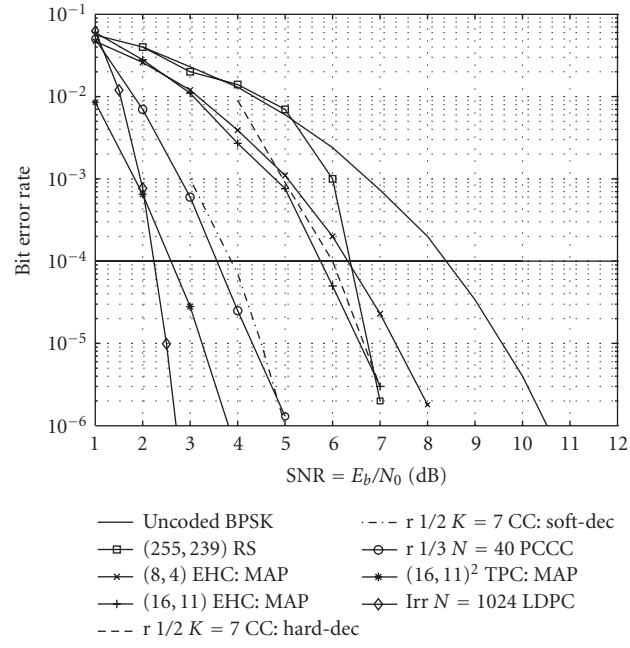

Figure 1: BER performance versus SNR for several error-correcting codes.

for all encoded bits. Note that the SNR = E_b/N_0 in dB is an energy ratio, rather than the power ratio S/N. The received energy per bit E_b is energy per symbol over code rate E_s/R, with constant E_s, and N_0 is the noise power spectral density. The thick black line indicates a BER of 10^{-4}; the coding gain for each code at this BER is easy to determine.

Three block codes are shown: a $(255, 239, 17)$ Reed-Solomon code, an $(8, 4, 4)$ extended Hamming code, and a $(16, 11, 4)$ extended Hamming code. Note that the longer extended Hamming code provides better performance due to its longer length. The Reed-Solomon code does not provide better performance until a much lower BER, even though it is significantly longer and has a better minimum distance, due to its higher rate.

Two convolutional codes, both rate 1/2 64-state constraint length 7, are compared [45]. One uses a hard-decision Viterbi decoder and the other uses a soft-decision Viterbi decoder. The soft-decision decoder performs about 2 dB better than the hard-decision decoder.

Three iteratively decoded codes are displayed as well, and the power of iterative decoding is clearly shown. These three codes provide the best performance on the graph. The parallel concatenated convolutional code (PCCC) is a classic turbo code, and used in the 3 GPP standard, although it is short; it has an interleaver and information sequence size of 40 bits, with a codeword length of 132 bits [46]. The $(16, 11)^2$ turbo product code is composed of component (16,11) extended Hamming codes, decoded with MAP decoding [47]. The rate 1/2 length 1024 irregular LDPC is similar to the code implemented in [48], with 64 decoding iterations used.

The use of ECC can allow a system to operate at significantly lower SNR than an uncoded system, for the same BER.

Whether this coding gain $\mathrm{ECC}_{\mathrm{gain}} = \mathrm{SNR}_U - \mathrm{SNR}_{\mathrm{ECC}}$ provides sufficient energy savings due to the lowered minimum transmitted power requirement to outweigh the cost of extra power consumption due to the decoder will be examined in the next section.

4. ENERGY SAVINGS FROM ECC

4.1. Minimum required transmit power

For an uncoded system, the minimum required transmit power $P_{\mathrm{TX},U}$ at the signal-to-noise ratio (termed SNR_U) required to achieve a desired BER is found from (4) and (7) to be

$$P_{\mathrm{TX},U}[W] = \eta_U \frac{E_b}{N_0} N \left(\frac{4\pi}{\lambda}\right)^2 d^n,$$
$$P_{\mathrm{TX},U}[W] = \eta_U 10^{(\mathrm{SNR}_U/10+\mathrm{RNF}/10)} (kTB) \left(\frac{4\pi}{\lambda}\right)^2 d^n, \tag{10}$$

where η_U is the uncoded system's spectral efficiency. RNF is the receiver noise figure in dB and SNR_U is the required SNR $= E_b/N_0$ in dB to achieve the target BER with an uncoded system. The path loss exponent n depends on the environment. At the frequencies of interest, $d > \lambda$ as stated in Section 2.2, so the far-field approximation of (8) is valid.

The uncoded system has a transmission rate R and bandwidth B, so the uncoded spectral efficiency $\eta_U = R/B$. We consider BPSK-modulated transmission, which has a maximum possible spectral efficiency of $\eta_{\max} = 1$, and so we require that $B = R$ and $\eta_U = 1$.

For an equal comparison, we require that the coded system also have an information transmission rate R. Recall that the information bits are the uncoded bits before going into the encoder, and the coded bits are the bits output from the encoder. The number of coded bits is greater than the number of information bits, so it would be an unfair comparison to consider the coded system to have a coded transmission rate of R, as then the information transmission rate would decrease to $R{*}R_C$. The code rate R_C is the number of information bits divided by the number of codeword bits. This means the uncoded system would be decoding R information bits per second, assuming BPSK modulation, while the coded system would decode only $R{*}R_C$ information bits per second. This would give the coded system an unfair advantage. Thus we require that the coded system transmit at an information transmission rate of R, as for the uncoded system.

The coded transmission rate or coded channel throughput R' then increases to $R' = R/R_C$, for a code of rate R_C. The bandwidth of the coded system, B_C, is assumed to increase with the coded transmission rate, so that $B_C = R'$. Thus the coded system's spectral efficiency decreases to $\eta_C = R/B_C = R_C$.

Minimizing transmit power is considered herein to be the most critical parameter for a low-power WSN, whose battery lifetime is dependent on power consumption. Therefore all transmit power and energy calculations use the minimum required transmit power and energy. In a low-power WSN scenario, transmitting with as much power as possible, up to regulatory limits, is not desirable. Rather, transmitting with as little power as possible, so as to extend sensor battery life, while maintaining a minimum required SNR, is our goal. Similar to a deep-space satellite scenario, the low-power WSN is far more power-constrained than bandwidth-constrained. In order to achieve power efficiency, we are willing to sacrifice spectral efficiency.

An equation similar to (10), but for the minimum required transmit power $P_{\mathrm{TX,ECC}}$ using ECC, can be found. Recall that the required $\mathrm{SNR}_{\mathrm{ECC}}$ is less than SNR_U by the coding gain $\mathrm{ECC}_{\mathrm{gain}}$. Also note that $\eta_C B_C = R$ and $\eta_U B = R$. The minimum required transmit power when using ECC, $P_{\mathrm{TX,ECC}}$, is given by

$$P_{\mathrm{TX,ECC}}[W] = \eta_C 10^{(\mathrm{SNR}_{\mathrm{ECC}}/10+\mathrm{RNF}/10)} kTB_C \left(\frac{4\pi}{\lambda}\right)^2 d^n,$$
$$P_{\mathrm{TX,ECC}}[W] = \frac{\eta_C B_C}{\eta_U B} \frac{P_{\mathrm{TX},U}}{10^{\mathrm{ECC}_{\mathrm{gain}}/10}} = \frac{P_{\mathrm{TX},U}}{10^{\mathrm{ECC}_{\mathrm{gain}}/10}}. \tag{11}$$

The required transmit power P_{TX} is converted to required transmit energy per transmitted information bit by dividing P_{TX} by the information transmission rate R in bps to obtain $Eb_{\mathrm{TX}} = P_{\mathrm{TX}}/R$ in J/bit. Since the information transmission rate R is the same for both uncoded and coded systems, the ratio of uncoded to coded energy per transmitted bit remains the same as for power. The information rate R is also assumed constant over all transmission distances d. This allows for a straightforward comparison of the minimum required transmit energy and power of coded and uncoded systems at different distances.

The transmit energy savings per information bit of the coded system is found as the difference between the minimum required transmit energy per information bit for uncoded and coded systems, as

$$Eb_{\mathrm{TX},U}[J/\mathrm{bit}] = \frac{P_{\mathrm{TX},U}}{R},$$
$$Eb_{\mathrm{TX,ECC}}[J/\mathrm{bit}] = \frac{P_{\mathrm{TX,ECC}}}{R} = \frac{Eb_{\mathrm{TX},U}}{10^{\mathrm{ECC}_{\mathrm{gain}}/10}}, \tag{12}$$
$$Eb_{\mathrm{TX},U} - Eb_{\mathrm{TX,ECC}} = Eb_{\mathrm{TX},U}\left(1 - 10^{-\mathrm{ECC}_{\mathrm{gain}}/10}\right).$$

Use of ECC lowers the required minimum transmit power and energy per decoded bit as a result of the coding gain $\mathrm{ECC}_{\mathrm{gain}}$. However, at the receiver, the coded system has the added power consumption of its decoder, which must be factored in as a cost of using ECC. We do not consider the additional power consumed by the encoder; typically the encoder is much smaller and consumes significantly less power than the decoder.

Decoder implementation results usually present one or two power consumption measurements at specified throughputs. We can factor in the cost of the decoder power consumption by taking the power consumption value at an

information throughput equal to the information transmission rate R, and dividing the power consumption by the throughput R to get energy per decoded bit Eb_{dec}. However, the power consumption values available for the implementations are almost always for high throughput. A model is needed to estimate the decoder power consumed at throughput below that measured, based on the available power consumption data.

4.2. Decoder power consumption

The power consumption of a digital CMOS decoder consists of two types: dynamic and static. Dynamic power consumption is primarily due, in CMOS logic, to the switching capacitance, and is modeled as $P_d \approx CV_{\text{dd}}^2 f$, where C is the total switched capacitance, V_{dd} is the power supply voltage, and f is the operating, or clock, frequency. The static power consumption is due to leakage current and DC biasing sources, and can be modeled as $P_s = I_{\text{leak}} V_{\text{dd}}$, where I_{leak} is the leakage current. The total power consumption is modeled as [49]

$$P_{\text{total}} = P_d + P_s \approx CV_{\text{dd}}^2 f + I_{\text{leak}} V_{\text{dd}}. \tag{13}$$

The dynamic power consumption increases linearly with frequency, and becomes the dominant factor at higher frequencies. At low frequencies, static power consumption dominates and the total power consumption no longer increases linearly with frequency, but approaches the static value. This is seen from the total power consumption model as

$$P_{\text{total}}(f) \approx af + b, \quad a = CV_{\text{dd}}^2,\ b = I_{\text{leak}} V_{\text{dd}}. \tag{14}$$

The decoder throughput R is proportional to f over most of the range of f, so the total power $P_{\text{total}} \propto aR + b$. At high frequencies, near the limit of the clocking frequency, the dynamic power will increase superlinearly with f, and the chip dissipates large amounts of power. We will not consider operation near the high-frequency limits of chip performance.

Figure 2 shows actual power versus throughput measurements for a digital implementation of a length 1024 rate 1/2 LDPC decoder incorporating the sum-product algorithm (SPA) [48]. A linear approximation for the normalized power is compared to the actual measurement data. The linear approximation is quite accurate in the linear, dynamic-power-dominated region of the power versus throughput curve.

From the decoder power consumption approximation, the energy cost per decoded information bit could be found as $Eb_{\text{dec}} = P_{\text{total}}/R$.

There is an additional factor to consider in power consumption, which is the implementation process. The decoder implementations presented in Table 1 span several different CMOS processes: from 0.5 μm to 0.16 μm. Larger processes have higher supply voltage and dissipate greater amounts of power. So as not to unfairly penalize decoders implemented in a larger process size, we scale the energy per decoded bit by V_{dd}^2. This results in an energy per decoded information bit Eb_{dec}, normalized to a supply voltage of 1 V, as

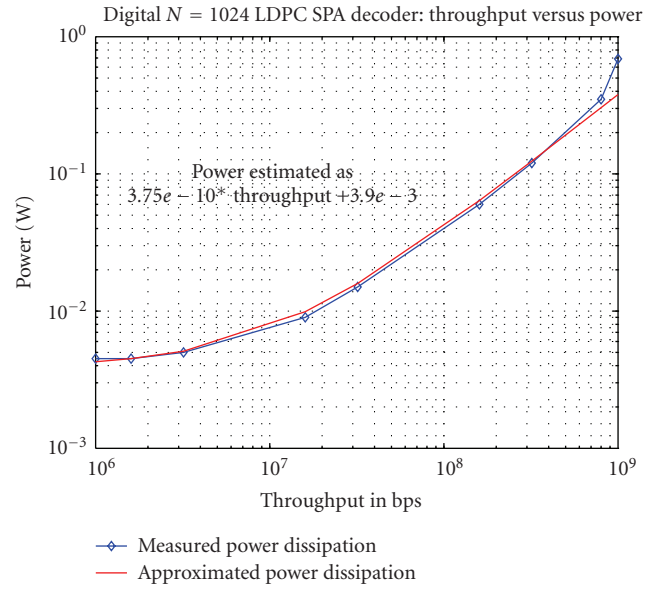

Figure 2: Power versus throughput: measured values and linear approximation for digital LDPC implementation.

$$Eb_{\text{dec}} = \frac{P_{\text{total}}}{RV_{\text{dd}}^2}. \tag{15}$$

When operating anywhere in the dynamic power/high throughput region, the energy per decoded information bit is constant at

$$Eb_{\text{dec}} = \frac{P_{\max}}{R_{\max} V_{\text{dd}}^2}. \tag{16}$$

This paper also considers analog decoder implementations, which use very small bias currents, so that the transistors operate in the subthreshold region. Hence, analog decoders inherently have very low power dissipation, and would seem a good choice for power-limited applications such as wireless sensor networks.

4.3. Energy savings of ECC and critical distance

The total energy cost or gain of using ECC with a particular decoder implementation, at a given frequency, distance, throughput, and required BER, may then be found as the combination of its energy savings due to coding gain from (12), plus the energy cost due to decoder power consumption as (15). This energy savings ΔES with respect to an uncoded system is found as the difference in minimum transmitted energy per information bit between uncoded and coded, minus the additional energy cost at the decoder. Recall that

Table 1: Different decoder implementations: coding gain, maximum measured core power consumption and information throughput, and energy per decoded information bit, normalized to $V_{dd} = 1$, at maximum measured power and throughput.

Decoder implementation	Coding gain in dB	P_{max} in mW	R_{max} in Mbps	V_{dd} in V	Eb_{dec} in nJ/bit	Process size in μm
(255,239) RS digital	2	58	160	1.8	0.1193	0.18
Digital rate 1/2 CC hard-dec Viterbi	2.3	85	106	1.8	0.2475	0.18
Digital rate 1/2 CC soft-dec Viterbi	4.2	83	67	2.2	0.1138	0.35
(8,4) EHC analog	2	0.15	3.7	0.8	0.0633	0.18
(16,11) EHC analog	2.6	2.7	135	1.8	0.0062	0.18
$(16, 11)^2$ TPC analog	5.7	86.1	1000	1.8	0.0266	0.18
Rate 1/3 turbo analog	4.8	4.1	2	2	0.5125	0.35
$N = 1024$ LDPC digital	6.1	630	500	1.5	0.56	0.16
(32,8,10) LDPC analog	1.3	5	80	1.8	0.0193	0.18

$B = R$. The energy savings ΔES is given by

$$\begin{aligned}\Delta ES &= Eb_{TX,U} - Eb_{TX,ECC} - Eb_{dec} \\ &= \frac{P_{TX,U}}{R}\left(1 - 10^{-ECC_{gain}/10}\right) - Eb_{dec} \\ &= \frac{10^{(SNR_U/10+RNF/10)}kTB}{R}\left(\frac{4\pi}{\lambda}\right)^2 d^n\left(1 - 10^{-ECC_{gain}/10}\right) \\ &\quad - \frac{P_{total}}{RV_{dd}^2}, \\ \Delta ES &= 10^{(SNR_U/10+RNF/10)}kT\left(\frac{4\pi}{\lambda}\right)^2 d^n\left(1 - 10^{-ECC_{gain}/10}\right) \\ &\quad - \frac{P_{total}}{RV_{dd}^2}.\end{aligned} \tag{17}$$

The distance d at which $\Delta ES = 0$ is termed the critical distance d_{CR}. This is the distance at which use of a particular decoder implementation becomes energy-efficient. For sensors greater than a distance d_{CR} apart, use of that decoder implementation saves energy compared to an uncoded system. The critical distance d_{CR} is found from (17) as

$$d_{CR} = \left(\frac{P_{total}}{10^{(SNR_U/10+RNF/10)}kTRV_{dd}^2\left(1 - 10^{-ECC_{gain}/10}\right)}\left(\frac{\lambda}{4\pi}\right)^2\right)^{1/n}. \tag{18}$$

P_{total} is represented as a linear function of the throughput R, as $P_{total} = P_{max} * R/R_{max}$. Recall that P_{max} and R_{max} are the maximum measured power and throughput values, respectively, and they fall within the decoder's dynamic power consumption region. The static power contribution is considered to be negligible in the dynamic region. The factor of $(1/R)^{1/n}$ in (18) will be canceled, in the dynamic region, by R in P_{total}. Thus d_{CR} in the dynamic region is independent of throughput, and has constant value. The critical distance is given by

$$d_{CR} = \left(\frac{P_{max}}{10^{(SNR_U/10+RNF/10)}kTR_{max}V_{dd}^2\left(1 - 10^{-ECC_{gain}/10}\right)}\left(\frac{\lambda}{4\pi}\right)^2\right)^{1/n}. \tag{19}$$

For a low throughput channel, we need to consider the type of network traffic across the channel. Bursty traffic, where long periods of silence are interspersed with brief bursts of data, is representative of many types of low throughput networks. Examples are weather sensors or patient temperature sensors reporting conditions at fixed intervals, or sensors receiving data from security cameras at an isolated facility that only transmit data when there is movement or pixel change. Bursty traffic channels, while on average low throughput, are better represented as a channel which has high throughput for a certain percentage of time, and no throughput the rest of the time.

In the bursty traffic scenario, a low throughput channel of rate R is viewed as having high throughput or transmission rate $R_1 > R$ for $100h\%$ of the time, where $0 \le h \le 1$, and no throughput $100(1 - h)\%$ of the time, such that $hR_1 = R$. The decoder is assumed to be powered down during periods of no throughput. During the time when the decoder is operating, throughput is high and decoder power consumption follows the dynamic power consumption model. Averaged over time, the total decoder power consumption is found to be

$$P_{total} = \frac{hR_1P_{max}}{R_{max}} = \frac{RP_{max}}{R_{max}}, \tag{20}$$

the same as for the dynamic power consumption case. In other words, bursty traffic effectively lowers the dynamic power region to lower throughputs, because the data itself is delivered at a transmission rate within the dynamic power region.

Thus the critical distance d_{CR} for low throughput with bursty traffic is the same as (19). We will not consider a constant low throughput channel, as it is not an energy-efficient method of operating the decoder.

Another factor to consider is whether the minimum required uncoded transmit power, $P_{TX,U}$, exceeds regulatory limits on maximum allowable transmitted power at a certain distance $d_{P_{lim}} \leq d_{CR}$. If so, then coding will be necessary simply to reduce the transmit power below regulatory limits. The critical distance d_{CR} for the coded system would then drop to $d_{P_{lim}}$, provided that the minimum coded transmit power $P_{TX,ECC}$ did not also exceed the maximum power limitation.

There are many different regulatory limits, depending on location, frequency, and application. Thus it is not within the scope of this paper to determine whether $P_{TX,U}$ exceeds all possible limits at each frequency, application, and critical distance. However, this is a factor which should be considered for actual usage.

The next section considers both digital and analog decoder implementations and determines their critical distances at various frequencies and environments. Path loss exponents range from $n = 2$ for free space to $n = 4$ for office space with many obstacles and ranging over multiple floors. Both high and bursty traffic low throughput channels are considered.

5. CRITICAL DISTANCE RESULTS FOR IMPLEMENTED DECODERS

5.1. Decoder implementations

We now examine several different decoder implementations, both analog and digital, for a variety of code types. BPSK transmission over an AWGN channel is assumed for all decoders. Block codes considered include a high-rate digital $(255, 239)$ Reed-Solomon decoder [50], an analog $(8, 4, 4)$ extended Hamming decoder [51] and an analog $(16, 11, 4)$ extended Hamming decoder [47]. Two digital convolutional decoders are included, a hard-decision Viterbi [52] and a soft-decision Viterbi decoder [53]. Both decoders use a rate 1/2, 64-state, constraint length $K = 7$ convolutional code. Iterative decoders are examined as well. An analog rate 1/3 length 132 turbo decoder with interleaver size 40 [46] is considered, as well as an analog $(16, 11)^2$ turbo product decoder [47, 54] using MAP decoding on each component $(16, 11)$ extended Hamming codes. Two LDPC decoders are evaluated, a digital rate 1/2 length 1024 irregular LDPC sum-product decoder [48] and an analog rate 1/4 (32,8,10) regular LDPC min-sum decoder [55].

Table 1 displays the pertinent data for each decoder, including coding gain in dB, maximum measured decoder core power consumption P_{max}, corresponding maximum measured information (not coded) throughput R_{max}, core supply voltage V_{dd}. The decoded energy per information bit, Eb_{dec}, is found with (15), and assumes operation in either the dynamic power consumption region or a bursty traffic low throughput scenario, which is modeled equivalently to the dynamic region. The coding gain is compared to uncoded BPSK at a BER of 10^{-4}, and is the coding gain of the implemented decoder. The process size for each decoder is also presented. As shown, the analog decoders have the lowest Eb_{dec} values.

Table 2: Parameters used in critical distance calculations.

Path loss exponent	$n = 2, 3, 4$
Frequency range	450 MHz–10 GHz
Required BER	10^{-4}
Uncoded SNR (E_b/N_0)	8.3 dB
Receiver noise figure	5 dB [56]
Temperature	300 K

5.2. Critical distance values

From the energy per decoded data bit, Eb_{dec}, the critical distance d_{CR} for each decoder implementation may be found according to (19) for a variety of scenarios.

If we consider either a high throughput channel or a bursty traffic low throughput channel, then d_{CR}, found from (19), is independent of the throughput, with a single value regardless of throughput.

First we consider the path loss exponent n, as representative of the transmission environment. We examine d_{CR} for $n = 2$, as a free space, line-of-sight (LOS) model, either outdoors or in a hallway; $n = 3$ as an interior environment such as an office building, where the network is all located on the same floor, or an outdoor environment such as forest or foliated urban/suburban locations; and $n = 4$ as an interior environment with many obstructions and possibly multiple floors, or a dense urban environment. A frequency range from 450 MHz to 10 GHz is considered. Throughput is assumed to be either within the dynamic power region or low but bursty, and the critical distance d_{CR} is calculated according to (19). The parameters used in (19) are displayed in Table 2.

Figure 3 shows d_{CR} versus frequency for $n = 2$, free space path loss, for all decoders in Table 1. The decoder curves are shown in the order in which they appear in the graph legend, that is, top first.

At 10 GHz, the lowest critical distances belong to the analog (16,11) extended Hamming and $(16, 11)^2$ turbo product decoders, at 30 and 48 m, respectively. These decoders would be practical in an indoor hallway scenario, where sensors placed at ends of the hallway would have LOS.

At lower frequencies, the values of d_{CR} in a free space environment, assuming no interference or extra background noise, are extremely large. Not until $f = 3$ GHz do any of the critical distances drop below 100 m. For an outdoor scenario where sensors are very widely spaced, with an LOS component, perhaps for either infrequently located security sensors around a large perimeter, along a highway or railroad track, monitoring outdoor weather data, or monitoring a fault line, the large distances even at lower frequencies might be practical. The distances are far too large for any indoor scenario.

Figure 4 shows d_{CR} versus frequency for $n = 3$, an office environment or foliated outdoor environment.

The analog decoders could be practical, at the higher frequencies, for security scenarios where one might have security sensors spaced every few houses in an urban environment, or sensors placed in every few rooms of a hotel or office building. The analog (16,11) extended Hamming and

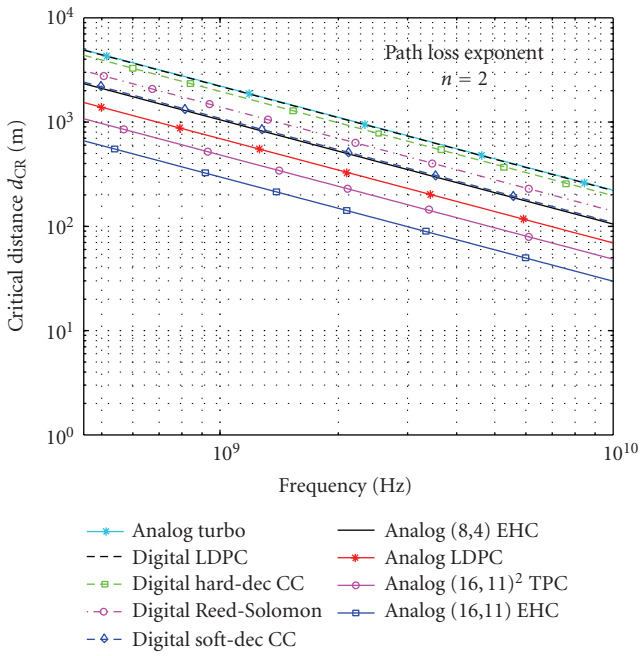

FIGURE 3: Estimated critical distance d_{CR} versus f for $n = 2$ free space path loss and high throughput or bursty low throughput channel.

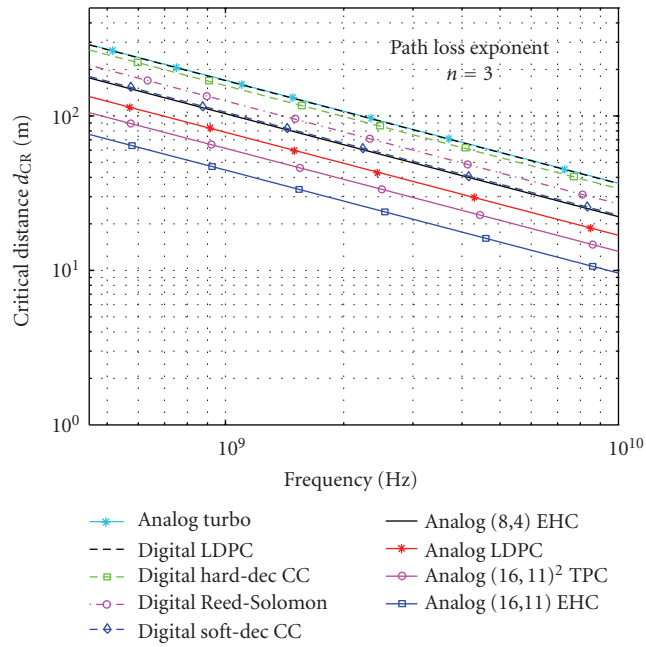

FIGURE 4: Estimated critical distance d_{CR} versus f for $n = 3$ path loss exponent and high throughput or bursty low throughput channel.

$(16, 11)^2$ turbo product decoders again have the lowest critical distances, at 15 m and 21 m, respectively, for $f = 5$ GHz, and 10 and 13 m at 10 GHz.

At the lowest frequency of 450 MHz, the lowest critical distance is 76 m for the (16,11) extended Hamming decoder, but all other decoders have critical distances above 100 m. Urban and suburban nodes which are not LOS, such as low buildings located more than a block apart, could be separated by distances greater than the critical distances even at the lowest frequencies, and well above the 2.4 GHz values. Outdoor sensor networks in forested regions monitoring nesting sites, or forest health and dryness, or avalanche-prone regions, could also be spaced further apart than the critical distances at low frequencies.

Figure 5 shows d_{CR} versus frequency for $n = 4$, either an office floor with many obstructions or between multiple floors, or a dense outdoor urban environment.

Critical distances, even at the lowest frequencies, are practical for a dense outdoor urban environment without LOS, for all decoders, as long as the sensors are spaced a few buildings apart.

For the office environment, the critical distance values are more practical for frequencies of 2 GHz and above. The analog decoders, with the exception of the analog turbo decoder, all have critical distances below 25 m at 2 GHz, and 10 m or less at 10 GHz. The analog (16,11) extended Hamming and $(16, 11)^2$ turbo product decoders again perform the best, with respective d_{CR} values at 10 GHz of 5.5 m and 7 m, at 5 GHz of 8 and 10 m, and at 2.4 GHz of 12 and 15.5 m. These distances could represent a sensor network monitoring different floors of a building, with a node in each office, or a network monitoring separate enclosures in an animal park.

These distances are just feasible, at the higher frequencies, to consider a sensor network for monitoring patients in a hospital. However, with additional interference and background noise, as would be likely in these environments, d_{CR} would certainly decrease, increasing the energy efficiency of each decoder implementation and making ECC more practical for this scenario.

The analog decoders, with their extremely low power consumption, provide the most energy-efficient decoding solution in these scenarios, except for the analog turbo decoder. The digital decoders all have higher d_{CR} values, from 2 to 4 times greater than the other analog decoders. For some scenarios, particularly free space transmission at frequencies below 1 GHz, ECC is not energy-efficient, except at very large distances. ECC is not always the best solution to minimizing energy. Our results for d_{CR} clearly show that energy-efficient use of ECC must consider the transmission environment and frequency, as well as decoder implementation. As the environment becomes more crowded, with more obstacles between sensor nodes, ECC becomes more energy-efficient at shorter distances. At the highest frequencies, ECC is practical for all the discussed scenarios when implemented with analog decoders.

5.3. Correction for power amplifier efficiency

Calculations presented so far have assumed that the power savings in RF transmitted power P_{TX} directly translate into savings of the DC chip power consumption P_{DC}. In practice

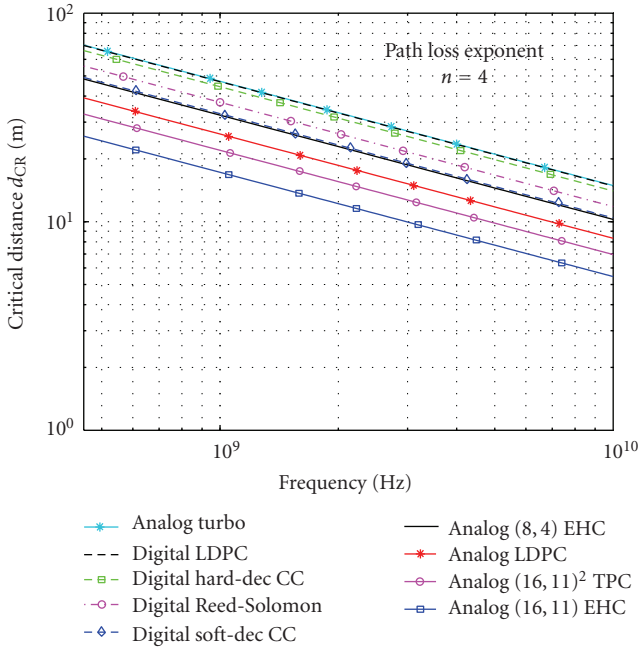

FIGURE 5: Estimated critical distance d_{CR} versus f for $n = 4$ path loss exponent and high throughput or bursty low throughput channel.

this assumption rarely holds true; in fact, both power factors are related through the power amplifier efficiency ε, defined as

$$\varepsilon = \frac{P_{TX}}{P_{DC}}. \tag{21}$$

Taking this into account, it is straightforward to show that (19), for high throughput or bursty traffic low throughput, needs to be modified as

$$d_{CR} = \left(\frac{\varepsilon P_{max}}{10^{(SNR_U/10+RNF/10)} kTR_{max} V_{dd}^2 (1-10^{-ECC_{gain}/10})} \left(\frac{\lambda}{4\pi}\right)^2 \right)^{1/n}, \quad R > R_d. \tag{22}$$

In order to use the above equation, power efficiency numbers for typical CMOS implementations need to be evaluated. As we will show below, ε varies from 19% to 65%, depending on what class power amplifier is used. The reasons for this wide spread of achieved efficiencies can be explained as follows. Contemporary standards such as 802.11 use digital modulation to achieve high spectral efficiency. For example, at 54 Mbps, WLAN uses 64-QAM modulation on each OFDM subcarrier [57], resulting in a transmit waveform with high peak-to-average ratio (PAR). A linear power amplifier must be used, which often has low power added efficiency (PAE), resulting in high power consumption.

One step towards more power efficient drivers is to use constant envelope modulation, as in the personal area network standard 802.15.4. Constant envelope transmitters can be driven closer to the compression point, resulting in a higher PAE; this in turn means lower power consumption. In this case, nonlinear (or switched-mode) power amplifiers may also be used, usually providing much higher efficiencies as a tradeoff for linearity. Typically, switched-mode amplifiers are also simpler in terms of realization complexity, warranting a more effective use of silicon area.

The highest efficiency of power amplification in silicon can be achieved using switched mode circuits [12]. Although theoretically, switched-mode PAs can transmit finite power with 100% efficiency, finite CMOS switching times and other effects result in lower efficiencies. As an example, a class E PA proposed in [58] has a PAE of 92.5% at an output power of −4.3 dBm in the 433 MHz ISM band using duty-cycle modulation (DCM). This efficiency figure, however, does not include the power consumption of the DCM circuit (which is effectively a preamplifier circuit). Taking this into account reduces the overall PAE to 65%, providing a better comparison towards other implementations. A somewhat comparable linear amplifier shown in [3] has a drain efficiency of 27.5% at an output power of −4.2 dBm at $f = 1.9$ GHz (however, a given drain efficiency will always be higher than the equivalent PAE).

Efficiency values for several types of power amplifiers are presented in Table 3. Their efficiency ε varies from 0.19, or 19%, to 0.65, with many common amplifier types showing ε near 0.3. At lower power output, as would be typical in a wireless sensor network, ε may drop even lower.

From (22), d_{CR} will change by $\varepsilon^{1/n}$, so assuming a power efficiency of 33% and free space path loss, d_{CR} will be 0.58 times the value obtained assuming ideal power efficiency of 100%. For $n = 3$, d_{CR} is 0.69 times the ideal power efficiency value of d_{CR}, and for $n = 4$, d_{CR} is 0.76 times the ideal power efficiency value. If we assume even lower power efficiency of 19%, d_{CR} reduces further to 0.44, 0.57, and 0.66 times its value calculated assuming ideal power efficiency, for $n = 2$, 3, and 4, respectively.

While these values do not drop d_{CR} dramatically, they do bring the $n = 4$ values at 10 GHz into the range of 3.5 to 7 m, and at 450 MHz to a range of 17 to 32 m, for the 4 most energy-efficient analog decoders with a power efficiency of 19%.

Figure 6 shows the changes in d_{CR} obtained assuming $\varepsilon = 0.33$ and 0.19, compared with ideal power efficiency of $\varepsilon = 1$, for the most energy-efficient decoder, the analog (16,11) extended Hamming decoder.

At $f = 10$ GHz, a power efficiency of 33% drops d_{CR} in free space from 30 m to 17 m, and 19% efficiency drops it further to 13 m. This is easily within the distance of one building to another, or from a house to a garage, for an LOS security scenario. With $n = 3$ and a power efficiency of 33%, d_{CR} falls from 9.5 m to 6.5 m, and to 5.5 m with a power efficiency of 19%. For $n = 4$ and power efficiency of 33%, d_{CR} is lowered from 5.5 m to 4 m, and power efficiency of 19% lowers it slightly further to 3.5 m. This is less than the distance between rooms in most buildings, making applications where a sensor in one room transmits to a receiver in another room behind it, perhaps for medical applications, practical for ECC using analog decoders at high frequencies.

Table 3: Comparison of various power amplifier configurations.

Description	Output power	Efficiency	Carrier frequency	Notes	Paper reference
Push-pull linear	−6.0 dBm	19%	900 MHz	Efficiency figure includes oscillator and frequency divider	[12]
Class B	9.8 dBm	38%	433 MHz	Includes 3 class A preamplifier stages	[14]
Class A/B	2.7 dBm	33%	1.9 GHz	N/A	[59]
Class E	−4.3 dBm	65%	433 MHz	Uses duty-cycle modulation	[58]
OOK cascode	−4.2 dBm	27.5%	1.9 GHz	N/A	[3]

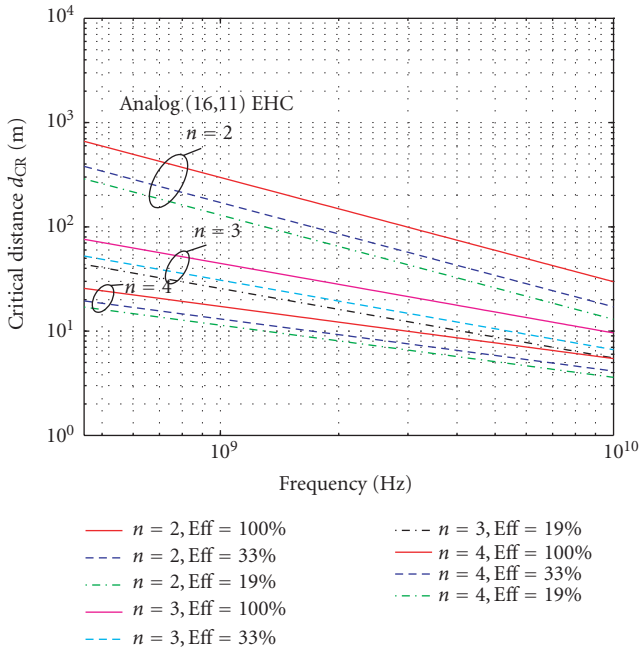

Figure 6: Estimated critical distance d_{CR} for analog (16,11) extended Hamming decoder assuming 19%, 33%, and 100% power efficiency, for $n = 2$, 3, and 4.

6. CONCLUSIONS

In free space line-of-sight scenarios, ECC is not very energy-efficient for frequencies below 2 GHz, except for widely spaced outdoor monitoring networks. In an urban outdoor setting, at higher frequencies, ECC can be practical for sensor networks placed between buildings, especially when implemented with analog decoders. For indoor environments, ECC is energy-efficient at high frequencies, for sensors placed at opposite ends of hallways or in adjacent rooms, or on multiple floors or in a dense urban environment at all frequencies. Analog decoders offer the most energy-efficient ECC solution, becoming energy-efficient at distances from 1/4 to 1/2 the critical distances of the digital decoders examined in this paper.

The effect of interference from other radiating sources has not been taken into account in this paper. This would reduce d_{CR} values, as the uncoded system must increase power to overcome the interference. The ECC system will thus become more energy-efficient at shorter distances when interference is considered.

The analog decoders in general, with their low power consumption, are better suited than digital decoders for the low-power requirements of wireless sensor networks. However, even the analog decoders require distances of 5–10 m (3.5–7 m for 19% power amplifier efficiency) at 10 GHz and $n = 4$ before they are energy-efficient in terms of the power the decoder consumes compared with the energy saved due to coding gain. Thus, analog decoders may not yet be practical for sensor network applications requiring close spacing of the sensors, such as monitoring patients in a crowded emergency room, babies in a nursery, or multiple sensors on one patient. Again, the effect of interference has not been considered, and in these scenarios where sensors are spaced closely together, interference could well be sufficient to require ECC for reliable operation.

The analog decoder critical distances considered for 10 GHz and $n = 4$ without interference are practical for sensors at ends of a room, or located one per room, such as air quality and temperature/humidity sensors, or sensors transmitting experimental data between university labs, or transmitting patient data during a procedure to equipment in another room.

Depending on the application and environment, analog decoders can be energy-efficient when used in a wireless sensor network. A combination of low power consumption and moderately high to high throughput makes analog decoders quite practical for WSN use. ECC is not always a practical solution for increasing link reliability, and as shown by the large critical distance values in free space at lower frequencies, an uncoded system may actually be more energy-efficient in certain environments, for specific applications. But in an office environment for communication between rooms, or a multiple-floor network, or security cameras in adjacent buildings, ECC, especially when implemented with analog decoders, can be a practical method of minimizing energy consumption in the wireless sensor network.

ACKNOWLEDGMENTS

Many thanks to Vincent Gaudet and Chris Winstead, for their helpful comments and suggestions regarding analog decoders and throughput, and to the editor and reviewers for their recommendations to improve the quality of this paper.

REFERENCES

[1] S. Roundy, B. Otis, Y. H. Chee, J. Rabaey, and P. Wright, "A 1.9GHz RF transmit beacon using environmentally scavenged energy," in *Proceedings of IEEE International Symposium on Low Power Electronics and Devices (ISLPED '03)*, Seoul, Korea, August 2003.

[2] T.-H. Lin, W. J. Kaiser, and G. J. Pottie, "Integrated low-power communication system design for wireless sensor networks," *IEEE Communications Magazine*, vol. 42, no. 12, pp. 142–150, 2004.

[3] B. Otis, Y. H. Chee, and J. Rabaey, "A 400 μW-RX, 1.6mW-TX super-regenerative transceiver for wireless sensor networks," in *Proceedings of IEEE International Solid-State Circuits Conference (ISSCC '05)*, vol. 1, pp. 396–397, San Francisco, Calif, USA, February 2005.

[4] K. Iniewski, C. Siu, S. Kilambi, et al., "Ultra-low-power circuit and system design tradeoffs for smart sensor network applications," in *Proceedings of the International Conference on Information and Communication Technology (ICICT '05)*, Cairo, Egypt, December 2005, invited paper.

[5] V. Ekanayake, C. Kelly IV, and R. Manohar, "An ultra-low-power processor for sensor networks," in *Proceedings of the 11th International Conference on Architectural Support for Programming Languages and Operating Systems (ASPLOS-XI '04)*, Boston, Mass, USA, October 2004.

[6] G. K. Ottman, H. F. Hofmann, and G. A. Lesieutre, "Optimized piezoelectric energy harvesting circuit using step-down converter in discontinuous conduction mode," *IEEE Transactions on Power Electronics*, vol. 18, no. 2, pp. 696–703, 2003.

[7] S. Roundy, D. Steingart, L. Fréchette, P. K. Wright, and J. Rabaey, "Power sources for wireless sensor networks," in *Proceedings of the 1st European Workshop on Wireless Sensor Networks (EWSN '04)*, pp. 1–17, Berlin, Germany, January 2004.

[8] W. Ye, J. Heidemann, and D. Estrin, "An energy-efficient MAC protocol for wireless sensor networks," in *Proceedings of 21st International Conference of IEEE Computer and Communications Societies (INFOCOM '02)*, vol. 3, pp. 1567–1576, New York, NY, USA, June 2002.

[9] K. Sohrabi and G. J. Pottie, "Performance of a novel self-organization protocol for wireless ad-hoc sensor networks," in *Proceedings of IEEE 50th Vehicular Technology Conference (VTC '99)*, vol. 2, pp. 1222–1226, Amsterdam, The Netherlands, September 1999.

[10] A. Woo and D. Culler, "A transmission control scheme for media access in sensor networks," in *Proceedings of ACM/IEEE International Conference on Mobile Computing and Networking (MOBICOM '01)*, Rome, Italy, July 2001.

[11] F. Bennett, D. Clarke, J. B. Evans, A. Hopper, A. Jones, and D. Leask, "Piconet: embedded mobile networking," *IEEE Personal Communications*, vol. 4, no. 5, pp. 8–15, 1997.

[12] A. Molnar, B. Lu, S. Lanzisera, B. W. Cook, and K. S. J. Pister, "An ultra-low power 900 MHz RF transceiver for wireless sensor networks," in *Proceedings of the IEEE on Custom Integrated Circuits Conference (CICC '04)*, pp. 401–404, Orlando, Fla, USA, October 2004.

[13] A.-S. Porret, T. Melly, D. Python, C. C. Enz, and E. A. Vittoz, "An ultralow-power UHF transceiver integrated in a standard digital CMOS process: architecture and receiver," *IEEE Journal of Solid-State Circuits*, vol. 36, no. 3, pp. 452–466, 2001.

[14] T. Melly, A.-S. Porret, C. C. Enz, and E. A. Vittoz, "An ultralow-power UHF transceiver integrated in a standard digital CMOS process: transmitter," *IEEE Journal of Solid-State Circuits*, vol. 36, no. 3, pp. 467–472, 2001.

[15] P. Lettieri, C. Fragouli, and M. B. Srivastava, "Low power error control for wireless links," in *Proceedings of the 3rd Annual ACM/IEEE International Conference on Mobile Computing and Networking (MOBICOM '97)*, pp. 139–150, Budapest, Hungary, September 1997.

[16] S. Mukhopadhyay, D. Panigrahi, and S. Dey, "Data aware, low cost error correction for wireless sensor networks," in *Proceedings of IEEE Wireless Communications and Networking Conference (WCNC '04)*, vol. 4, pp. 2492–2497, Atlanta, Ga, USA, March 2004.

[17] E. Shih, S. Cho, F. S. Lee, B. H. Calhoun, and A. Chandrakasan, "Design considerations for energy-efficient radios in wireless microsensor networks," *Journal of VLSI Signal Processing Systems for Signal, Image, and Video Technology*, vol. 37, no. 1, pp. 77–94, 2004.

[18] C. Berrou, A. Glavieux, and P. Thitimajshima, "Near Shannon limit error-correcting coding and decoding: turbo-codes," in *Proceedings of IEEE International Conference on Communications (ICC '93)*, vol. 2, pp. 1064–1070, Geneva, Switzerland, May 1993.

[19] R. G. Gallager, "Low-density parity-check codes," *IRE Transactions on Information Theory*, vol. 8, no. 1, pp. 21–28, 1962.

[20] S. Kasnavi, S. Kilambi, B. Crowley, K. Iniewski, and B. Kaminska, "Application of error control codes (ECC) in ultra-low-power RF transceivers," in *Proceedings of IEEE Dallas Circuits and Systems Workshop (DCAS '05)*, Dallas, Tex, USA, September 2005.

[21] N. Sadeghi, S. L. Howard, S. Kasnavi, K. Iniewski, V. C. Gaudet, and C. Schlegel, "Analysis of error control code use in ultra-low-power wireless sensor networks," in *Proceedings of IEEE International Symposium on Circuits and Systems (ISCAS '06)*, Kos, Greece, May 2006, accepted.

[22] C. Schlegel and L. Perez, *Trellis and Turbo Coding*, IEEE/Wiley, Piscataway, NJ, USA, 2004.

[23] B. Sklar, *Digital Communications: Fundamentals and Applications*, Prentice Hall, Englewood Cliffs, NJ, USA, 1988.

[24] W. L. Stutzman and G. A. Thiele, *Antenna Theory and Design*, John Wiley & Sons, New York, NY, USA, 2nd edition, 1998.

[25] T. S. Rappaport, *Wireless Communications: Principles and Practice*, Prentice Hall, Englewood Cliffs, NJ, USA, 1996.

[26] S. Y. Seidel and T. S. Rappaport, "Path loss prediction in multi-floored buildings at 914 MHz," *IEE Electronics Letters*, vol. 27, no. 15, pp. 1384–1387, 1991.

[27] C. Perez-Vega and J. L. Garcia, "A simple approach to a statistical path loss model for indoor communications," in *Proceedings of the 27th European Microwave Conference and Exhibition*, pp. 617–623, Jerusalem, Israel, September 1997.

[28] G. D. Durgin, T. S. Rappaport, and H. Xu, "Partition-based path loss analysis for in-home and residential areas at 5.85 GHz," in *Proceedings of IEEE Global Telecommunications Conference (GLOBECOM '98)*, vol. 2, pp. 904–909, Sydney, NSW, Australia, November 1998.

[29] D. B. Green and A. S. Obaidat, "An accurate line of sight propagation performance model for ad-hoc 802.11 wireless LAN (WLAN) devices," in *Proceedings of IEEE International*

Conference on Communications (ICC '02), vol. 5, pp. 3424–3428, New York, NY, USA, April-May 2002.

[30] J. Hansen and P. E. Leuthold, "The mean received power in ad hoc networks and its dependence on geometrical quantities," *IEEE Transactions on Antennas and Propagation*, vol. 51, no. 9, pp. 2413–2419, 2003.

[31] D. M. J. Devasirvatham, C. Banerjee, M. J. Krain, and D. A. Rappaport, "Multi-frequency radiowave propagation measurements in the portable radio environment," in *Proceedings of IEEE International Conference on Communications (ICC '90)*, vol. 4, pp. 1334–1340, Atlanta, Ga, USA, April 1990.

[32] T. J. Harrold, A. R. Nix, and M. A. Beach, "Propagation studies for mobile-to-mobile communications," in *Proceedings of IEEE 54th Vehicular Technology Conference (VTC '01)*, vol. 3, pp. 1251–1255, Atlantic City, NJ, USA, October 2001.

[33] H. Hashemi, "The indoor radio propagation channel," *Proceedings of the IEEE*, vol. 81, no. 7, pp. 941–968, 1993.

[34] J. Sydor, "True broadband for the countryside," *IEE Communications Engineer*, vol. 2, no. 2, pp. 32–36, 2004.

[35] A. Aguiar and J. Gross, "Wireless channel models," Tech. Rep. TKN-03-007, Telecommunications Networks Group, Technische Universität Berlin, Berlin, Germany, April 2003.

[36] R. W. Hamming, "Error detecting and error correcting codes," *The Bell System Technical Journal*, vol. 29, no. 2, pp. 147–160, 1950.

[37] I. S. Reed and G. Solomon, "Polynomial codes over certain finite fields," *SIAM Journal on Applied Mathematics*, vol. 8, pp. 300–304, 1960.

[38] R. C. Bose and D. K. Ray-Chaudhuri, "On a class of error correcting binary group codes," *Information and Control*, vol. 3, pp. 68–79, 1960.

[39] A. Hocquenghem, "Codes correcteurs d'erreurs," *Chiffres*, vol. 2, pp. 147–156, 1959.

[40] A. J. Viterbi, "Error bounds for convolutional codes and an asymptotically optimum decoding algorithm," *IEEE Transactions on Information Theory*, vol. 13, no. 2, pp. 260–269, 1967.

[41] L. R. Bahl, J. Cocke, F. Jelinek, and J. Raviv, "Optimal decoding of linear codes for minimizing symbol error rate," *IEEE Transactions on Information Theory*, vol. 20, no. 2, pp. 284–287, 1974.

[42] J. Pearl, *Probabilistic Reasoning in Intelligent Systems: Networks of Plausible Inference*, Morgan Kaufmann, San Mateo, Calif, USA, 1988.

[43] N. Wiberg, "Codes and decoding on general graphs," thesis of Doctor of Philosophy, Linköping University, Linköping, Sweden, 1996.

[44] M. P. C. Fossorier, M. Mihaljević, and H. Imai, "Reduced complexity iterative decoding of low-density parity check codes based on belief propagation," *IEEE Transactions on Communications*, vol. 47, no. 5, pp. 673–680, 1999.

[45] J. G. Proakis, *Digital Communications*, McGraw-Hill, New York, NY, USA, 4th edition, 2001.

[46] D. Vogrig, A. Gerosa, A. Neviani, A. Graell I Amat, G. Montorsi, and S. Benedetto, "A 0.35-μm CMOS analog turbo decoder for the 40-bit rate 1/3 UMTS channel code," *IEEE Journal of Solid-State Circuits*, vol. 40, no. 3, pp. 753–761, 2005.

[47] C. Winstead, "Analog Iterative Error Control Decoders," thesis of Doctor of Philosophy, Department of Electrical & Computer Engineering, University of Alberta, Alberta, Canada, 2004.

[48] A. J. Blanksby and C. J. Howland, "A 690-mW 1-Gb/s 1024-b, rate-1/2 low-density parity-check code decoder," *IEEE Journal of Solid-State Circuits*, vol. 37, no. 3, pp. 404–412, 2002.

[49] J. Rabaey, A. Chandrakasan, and B. Nikolic, *Digital Integrated Circuits*, Prentice Hall, Englewood Cliffs, NJ, USA, 2nd edition, 2003.

[50] T. S. Fill and P. G. Gulak, "An assessment of VLSI and embedded software implementations for Reed-Solomon decoders," in *Proceedings of IEEE Workshop on Signal Processing Systems (SIPS '02)*, pp. 99–102, San Diego, Calif, USA, October 2002.

[51] C. Winstead, N. Nguyen, V. C. Gaudet, and C. Schlegel, "Low-voltage CMOS circuits for analog iterative decoders," *IEEE Transactions on Circuits and Systems I: Regular Papers*, vol. 52, no. 4, 2005.

[52] M. Kawokgy, C. Andre, and T. Salama, "Low-power asynchronous Viterbi decoder for wireless applications," in *Proceedings of the International Symposium on Low Power Electronics and Design (ISLPED '04)*, pp. 286–289, Newport, Calif, USA, August 2004.

[53] C.-C. Lin, C.-C. Wu, and C.-Y. Lee, "A low power and high speed Viterbi decoder chip for WLAN applications," in *Proceedings of the 29th European Solid-State Circuits Conference (ESSCIRC '03)*, pp. 723–726, Lissabon, Portugal, September 2003.

[54] C. Winstead, C. Schlegel, and V. C. Gaudet, "CMOS analog decoder for (256,121) block turbo code," submitted to *EURASIP Journal on Wireless Communications and Networking*, special issue: CMOS RF circuits for wireless applications.

[55] S. Hemati, A. H. Banihashemi, and C. Plett, "An 80-Mb/s 0.18-μm CMOS analog min-sum iterative decoder for a (32,8,10) LDPC code," in *Proceedings of the IEEE Custom Integrated Circuits Conference (CICC '05)*, pp. 243–246, San Jose, Calif, USA, September 2005.

[56] T. Lee, *The Design of CMOS Radio-Frequency Integrated Circuits*, Cambridge University Press, Cambridge, UK, 2nd edition, 2004.

[57] "Wireless LAN medium access control (MAC) and physical layer (PHY) specification," *LAN MAN Standards Committee, IEEE Computer Society*, IEEE, New York, NY, USA, IEEE Std 802.11 - 1997 edition, 1997.

[58] D. Aksin, S. Gregori, and F. Maloberti, "High-efficiency power amplifier for wireless sensor networks," in *Proceedings of the IEEE International Symposium on Circuits and Systems (ISCAS '05)*, vol. 6, pp. 5898–5901, Kobe, Japan, May 2005.

[59] Y. H. Chee, J. Rabaey, and A. M. Niknejad, "A class A/B low power amplifier for wireless sensor networks," in *Proceedings of the IEEE International Symposium on Circuits and Systems (ISCAS '04)*, vol. 4, pp. 409–412, Vancouver, BC, Canada, May 2004.

Sheryl L. Howard received the B.S.E.E. degree in 1984 from the University of Utah, Salt Lake City, Utah, and the M.E.E.E. degree in 1988, also from the University of Utah. She is currently working towards the Ph.D. degree in electrical engineering at the University of Alberta, Edmonton, AB, Canada. Her research interests include iterative error control decoding and coding techniques.

Christian Schlegel received the Dipl. El. Ing. ETH degree from the Federal Institute of Technology, Zurich, in 1984, and the M.S. and Ph.D. degrees in electrical engineering from the University of Notre Dame, Notre Dame, Ind, in 1986 and 1989. He held academic positions at the University of South Australia, University of Texas, and University of Utah, Salt Lake City. In 2001 he was named iCORE Professor for High-Capacity Digital Communications at the University of Alberta, Canada, a 3-million-dollar research program in leading-edge digital communications. His interests are in error control coding and applications, multiple access communications, digital communications, and analog and digital implementations of communications systems. He is the author of *Trellis Coding* and *Trellis and Turbo Coding* by IEEE/Wiley, and *Coordinated Multiple User Communications*, coauthored with Professor Alex Grant. He received a 1997 Career Award, and a Canada Research Chair in 2001. He is an Associate Editor for coding theory and techniques for IEEE Transactions on Communications, and a Guest Editor of the IEEE Proceedings on Turbo Coding. He served as Technical Program Cochair of ITW '01 and ISIT '05, and General Chair of CTW '05, as well as on numerous technical conference program committees.

Kris Iniewski is an Associate Professor at the Electrical and Computer Engineering Department of University of Alberta. He is also a President of CMOS Emerging Technologies, Inc., a consulting company in Vancouver. His research interests are in advanced CMOS devices and circuits for ultra-low-power wireless systems, medical imaging, and optical networks. From 1995 to 2003, he was with PMC-Sierra and held various technical and management positions in research & development and strategic marketing. Prior to joining PMC-Sierra, from 1990 to 1994, he was an Assistant Professor at the University of Toronto's Electrical and Computer Engineering Department. He has published over 80 research papers in international journals and conferences. He holds 18 international patents granted in USA, Canada, France, Germany, and Japan. He is a frequent invited speaker and consults for multiple organizations internationally. He received his Ph.D. degree in electronics (with honors) from the Warsaw University of Technology (Warsaw, Poland) in 1988. Together with Carl McCrosky and Dan Minoli he is an author of *Data Networks-VLSI and Optical Fibre* (Wiley, 2006) and editor of *Emerging Wireless Technologies* (CRC Press, 2006).

Preliminary call for papers

The 2011 European Signal Processing Conference (EUSIPCO-2011) is the nineteenth in a series of conferences promoted by the European Association for Signal Processing (EURASIP, www.eurasip.org). This year edition will take place in Barcelona, capital city of Catalonia (Spain), and will be jointly organized by the Centre Tecnològic de Telecomunicacions de Catalunya (CTTC) and the Universitat Politècnica de Catalunya (UPC).

EUSIPCO-2011 will focus on key aspects of signal processing theory and applications as listed below. Acceptance of submissions will be based on quality, relevance and originality. Accepted papers will be published in the EUSIPCO proceedings and presented during the conference. Paper submissions, proposals for tutorials and proposals for special sessions are invited in, but not limited to, the following areas of interest.

Areas of Interest

- Audio and electro-acoustics.
- Design, implementation, and applications of signal processing systems.
- Multimedia signal processing and coding.
- Image and multidimensional signal processing.
- Signal detection and estimation.
- Sensor array and multi-channel signal processing.
- Sensor fusion in networked systems.
- Signal processing for communications.
- Medical imaging and image analysis.
- Non-stationary, non-linear and non-Gaussian signal processing.

Submissions

Procedures to submit a paper and proposals for special sessions and tutorials will be detailed at www.eusipco2011.org. Submitted papers must be camera-ready, no more than 5 pages long, and conforming to the standard specified on the EUSIPCO 2011 web site. First authors who are registered students can participate in the best student paper competition.

Important Deadlines:

Proposals for special sessions	15 Dec 2010
Proposals for tutorials	18 Feb 2011
Electronic submission of full papers	**21 Feb 2011**
Notification of acceptance	23 May 2011
Submission of camera-ready papers	6 Jun 2011

Webpage: www.eusipco2011.org

EURASIP
European Association for Signal Procesing

CTTC
Centre Tecnològic de Telecomunicacions de Catalunya

UPC